6-2022

# Mutations in Caveolin Binding Motif Alter Human Follicle Stimulating Hormone Receptor Signaling

Katarina Zahedi
*Union College - Schenectady, NY*

# Mutations in Caveolin Binding Motif Alter Human Follicle Stimulating Hormone Receptor Signaling

By

Katarina Zahedi

********

Submitted in partial fulfillment

of the requirements for

Honors in Department of Biochemistry

UNION COLLEGE

June, 2022

## ABSTRACT

Globally, there are about 48 million couples and 186 million individuals of reproductive age that are affected by infertility. Some cases of infertility in both men and women have been attributed to impaired follicle stimulating hormone (FSH) signaling. The lack of proper function of the cognate receptor for FSH (FSHR) could contribute to infertility since the biochemical signal generated by FSH binding to FSHR stimulates the production of a sperm-stabilizing protein in males and follicle maturation in females. It has been demonstrated that human FSHR (hFSHR) localizes to lipid rafts, which are rigid and detergent-resistant microdomains in the cell membrane. Their structure is in part due to having higher concentrations of cholesterol and sphingolipids compared to the surrounding plasma membrane. Additionally, some lipid rafts are characterized by the presence of the protein caveolin. Signaling pathways for some cell surface receptors have been demonstrated to be regulated by residency in lipid raft domains either by separating the related molecules inhibiting premature signaling or by colocalizing the related molecules to facilitate signaling. Based on evidence that FSHR forms direct protein-protein interactions with caveolin, it was hypothesized that disruption of the caveolin binding motif (CBM), a conserved peptide sequence present in proteins associated with caveolin, would affect hFSHR signaling. In hFSHR this sequence is found in transmembrane helix 4 between amino acids 479-489. The current study investigated the effect of mutations in the CBM on hFSHR signaling. The mutants were created via site-directed mutagenesis and expression vectors were transfected in HEK293 cells. Cells stably expressing the mutant FSHRs underwent western blot analysis for qualitative comparison of signaling. Mutations in three or four of the four conserved phenylalanine residues of the CBM resulted in much higher signaling compared to the wild-type and at a faster rate of activation. Elevated signaling at shorter FSH treatment times suggests that

the mutated receptor might be more sensitive to FSH and may hint at the role of the caveolin interaction in regulating hFSHR signaling. Because current infertility treatments are costly, tend to have low success rates, and are not accessible to everyone, a greater understanding of FSH signaling pathways could lead to the design of more successful infertility treatment methods.

## TABLE OF CONTENTS

# INTRODUCTION

Follitropin, or the follicle stimulating hormone (FSH), is a hormone secreted by gonadotroph cells in the anterior pituitary that plays a role in both male and female fertility (Figure 1).[1] Lack of proper FSH function causes reduced spermatogenesis thus impairing fertility in men and reduced folliculogenesis thus causing infertility in women.[2,3] Globally, there are about 48 million couples and 186 million individuals of reproductive age that are affected by infertility.[4] Although infertility can be treated with medication, surgery, intrauterine insemination, or assisted reproductive technology, these services are costly, tend to have low success rates, and are not accessible to everyone.[5] However, more successful infertility treatment methods could be designed if FSH signaling pathways were better understood.

The FSH receptor (FSHR) is a seven transmembrane domain G protein-coupled receptor (GPCR) located in the membrane of Sertoli cells in testes and granulosa cells in ovaries (Figure 2).[6] Lack of proper FSHR function and signaling could contribute to infertility since the biochemical signal generated by FSH binding to FSHR stimulates the production of a sperm-stabilizing protein in males and follicle maturation in females (Figure 3).[1] There are many signaling pathways for FSHR, where a mechanism for regulation of these signaling pathways is required, such as lipid rafts.

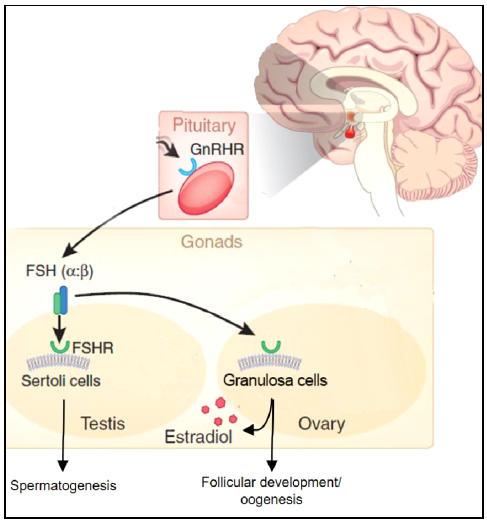


Figure 1. FSHR in HPG axis.[3]

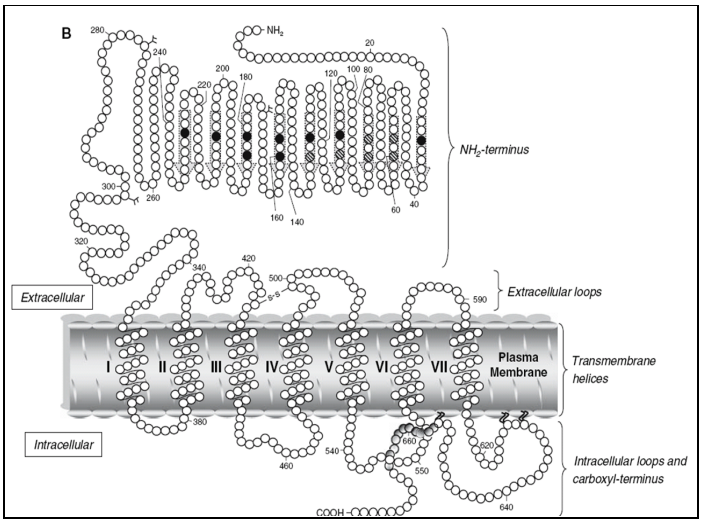


Figure 2. Extracellular, transmembrane, and intracellular Domains of FSHR.[6]

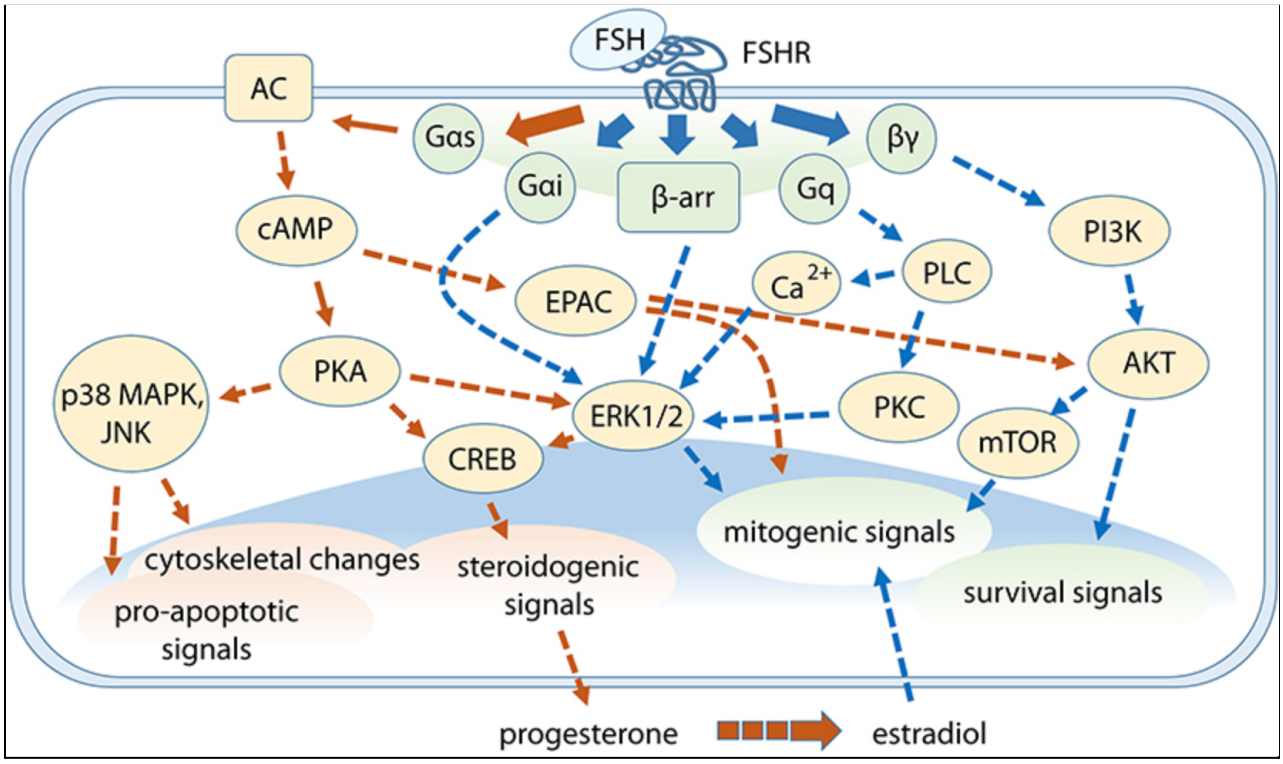


Figure 3. FSH activates FSH and other downstream signaling pathways.[7]

Human FSHR (hFSHR) localizes to lipid rafts, which are rigid and detergent-resistant microdomains in the cell membrane due to having higher concentrations of cholesterol and sphingomyelin compared to the surrounding plasma membrane (Figure 4).[8-10] Based on these

properties, lipid rafts can regulate receptor activity and their signal transduction pathway. By specifically studying the ERK 1/2 signaling pathway, also known as the p44/42 MAPK pathway, as mediated by the activation of beta-arrestin when FSH binds to FSHR, a greater understanding of how this signaling pathway affects the synthesis of vital sex steroids can be discovered.

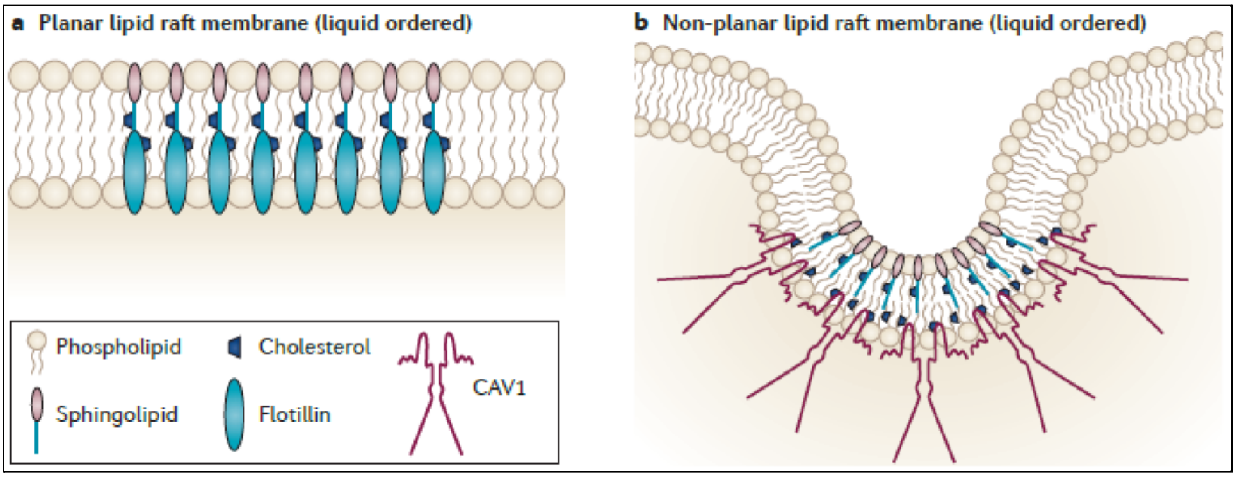


Figure 4. Schematic diagram of (A) lipid rafts and (B) caveolae, a specialized type of lipid raft. A key is shown indicating caveolin (CAV1) presence in caveolae.[11]

Some lipid rafts contain the protein caveolin, which localizes GPCRs to lipid rafts.[12] Caveolin is located within the caveolae, or the invaginated subdomains of the lipid raft.[13] Caveolin contains a caveolin scaffolding domain (CSD), which interacts with the caveolin binding motif (CBM) in target proteins.[13] Thus, caveolin is important in not only protein-lipid interactions in the raft but also protein-protein interactions. Because of the presence of caveolin and the composition of the lipid rafts, signaling pathways can be regulated at these locations, either by separating the related molecules thus inhibiting the signal or by colocalizing the related molecules thus stimulating signaling.[12]

Previous work in our lab suggests that FSHR forms direct protein-protein interactions with caveolin through the caveolin binding motif (CBM), which is a conserved peptide sequence

present in proteins associated with caveolin (Figure 5).[14] The canonical sequence of CBM is shown below as well as the corresponding sequence from hFSHR:

Caveolin Binding Motif

**Φ** X **Φ** X X X X **Φ** X X **Φ**

**F** A **F** A A A L **F** P I **F**

**479 481 486 489**

**(A) (B) (C) (D)**

The canonical sequence contains four aromatic residues (**Φ)** which could be the amino acids tryptophan, phenylalanine, or tyrosine. X represents any amino acid (which means they are probably not important to the CBM). Other studies have shown that variations in this motif and different structural conformations of the protein can negatively affect caveolin recognition, thereby preventing targeting of the protein to lipid rafts.[13] We hypothesize that disruption of the CBM in FSHR will prevent targeting to the raft and thus will affect signaling.

To test this hypothesis, the hFSHR CBM will be mutated, where aromatic residues, or phenylalanines (F), will be mutated to the amino acid leucine (L) to determine the importance of the phenylalanine residues.[14] **A** represents the point mutation F479L, **B** is F481L, **C** is F486L, **D** is F489L, and any combination of two or more letters represents a point mutation at those two or more locations. As seen in the helical peptide wheel, the amino acids at the A, C, and D locations may be located on the same side of the alpha helix while the amino acid at the B location may be located on the other side, thus suggesting a potential mechanism for how the FSHR interacts with caveolin (Figure 6). A relative solvent accessibility (RSA) model of FSHR confirms the presence of all four conserved phenylalanines in the CBM to be in the transmembrane domain, or completely buried away from solvent (Figure 7). To further visualize the CBM, a 3D predicted model of FSHR shows the four phenylalanine residues present in an alpha helix (Figure 8).

Proline is also present in the CBM, where proline has often been known to be a helix breaker. However, transmembrane domains usually exist as alpha helices, but the RSA model of FSHR predicts the proline residue to be completely buried within the transmembrane domain (Figure 7). Additionally, the proline residue is shown to not be in a helix in a 3D predicted model of FSHR, and is instead present in a loop/turn protein secondary structure (Figure 8). Thus, this proline residue within the CBM might also contribute to FSHR-caveolin interactions.

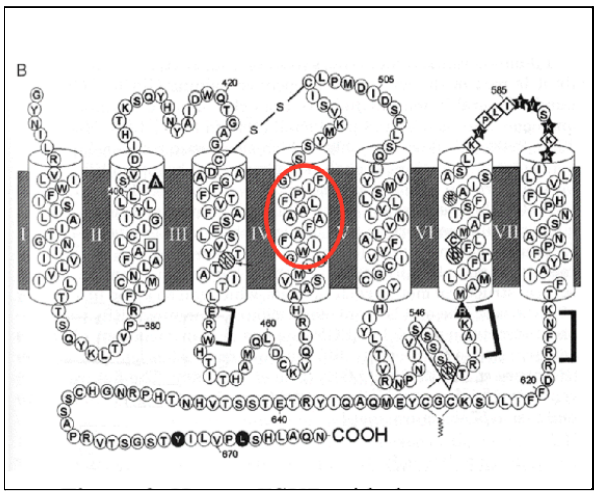


Figure 5. hFSHR in the cell membrane, with the combined caveolin binding motif circled in fourth transmembrane domain.[1]

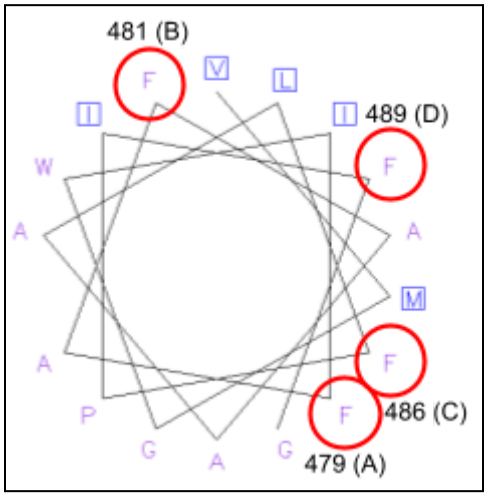


Figure 6. Helical wheel of amino acids in the caveolin binding motif (CBM), with the location of mutations circled in red.

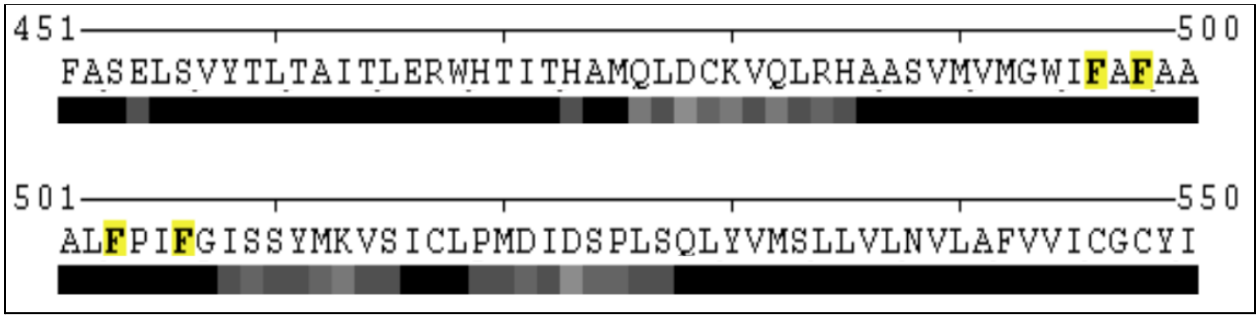


Figure 7. RSA model of FSHR CBM, where the phenylalanines (F) in the CBM are highlighted in yellow. The proline (P) is shown to be in an alpha helix and has an RSA score of 0 (0-9% RSA, represented by a black square), or completely buried from solvent.

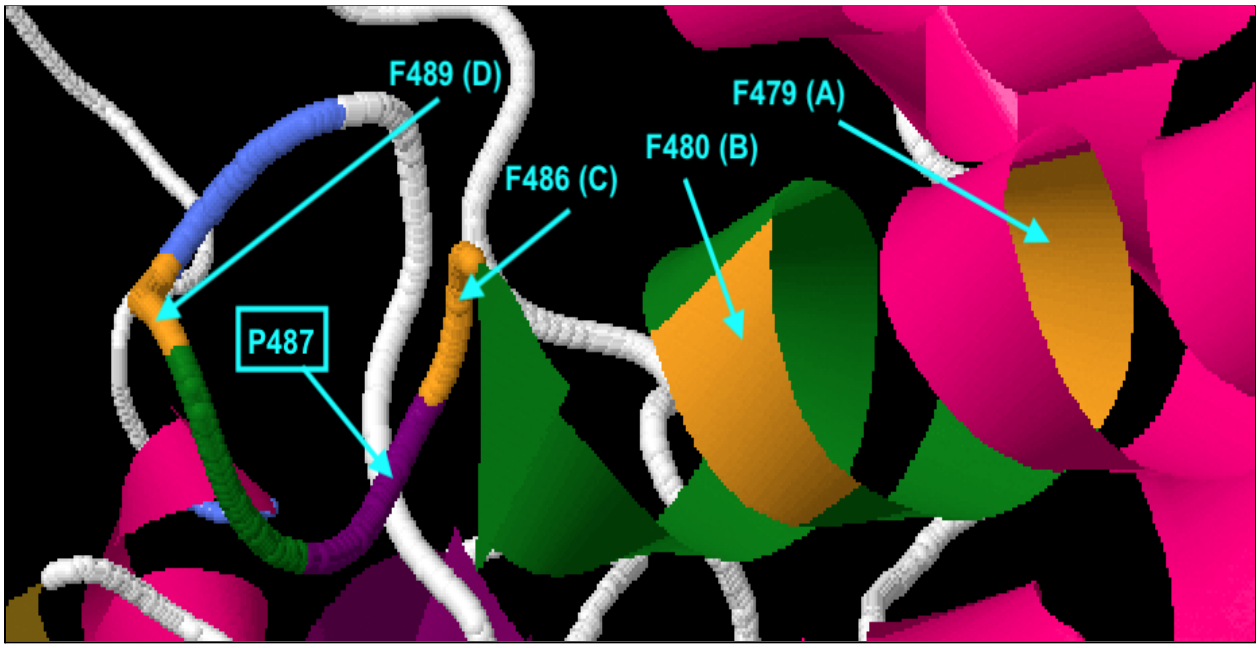

Figure 8. 3D predicted model of FSHR. Orange color indicates phenylalanines (F) in the CBM. Purple indicates the proline (P487) in the CBM.

By mutating the amino acid sequence and studying its effects on hFSHR signaling, the role of the CBM in FSHR interaction with caveolin can be better understood. Because our lab has previously shown that caveolin interacts with FSHR, we predict that mutating the CBM will affect hFSHR signaling. The research process to test this hypothesis has four stages: (1) designing a plan for generating expression vectors for the mutant hFSHRs, (2) generating the expression vectors for the mutant hFSHRs, (3) transfection and selection for cells stably expressing the mutant hFSHRs, and (4) testing how varying mutations in the hFSHR affects receptor presence, location, and function. To test this hypothesis, stably expressed ABCD, ABC, and BCD mutant cell lines were made and tested for changes in hFSHR signaling. Stably expressed AB, BC, and CD mutant cell lines were also generated for future signaling experiments.

Understanding the interaction between FSHR and caveolin can provide insight into FSHR function and defects in FSHR function leading to impaired fertility. By studying these mutants, the integral parts of the FSHR that promote receptor-caveolin interaction can be established. Thus, by having more knowledge about normal receptor function or what aspects must be mimicked for normal receptor function, agonists or antagonists that promote proper receptor function (proper receptor-caveolin interaction) can be developed as an assisted reproductive technology or a more accessible infertility treatment.

## METHODS

**Overview:**

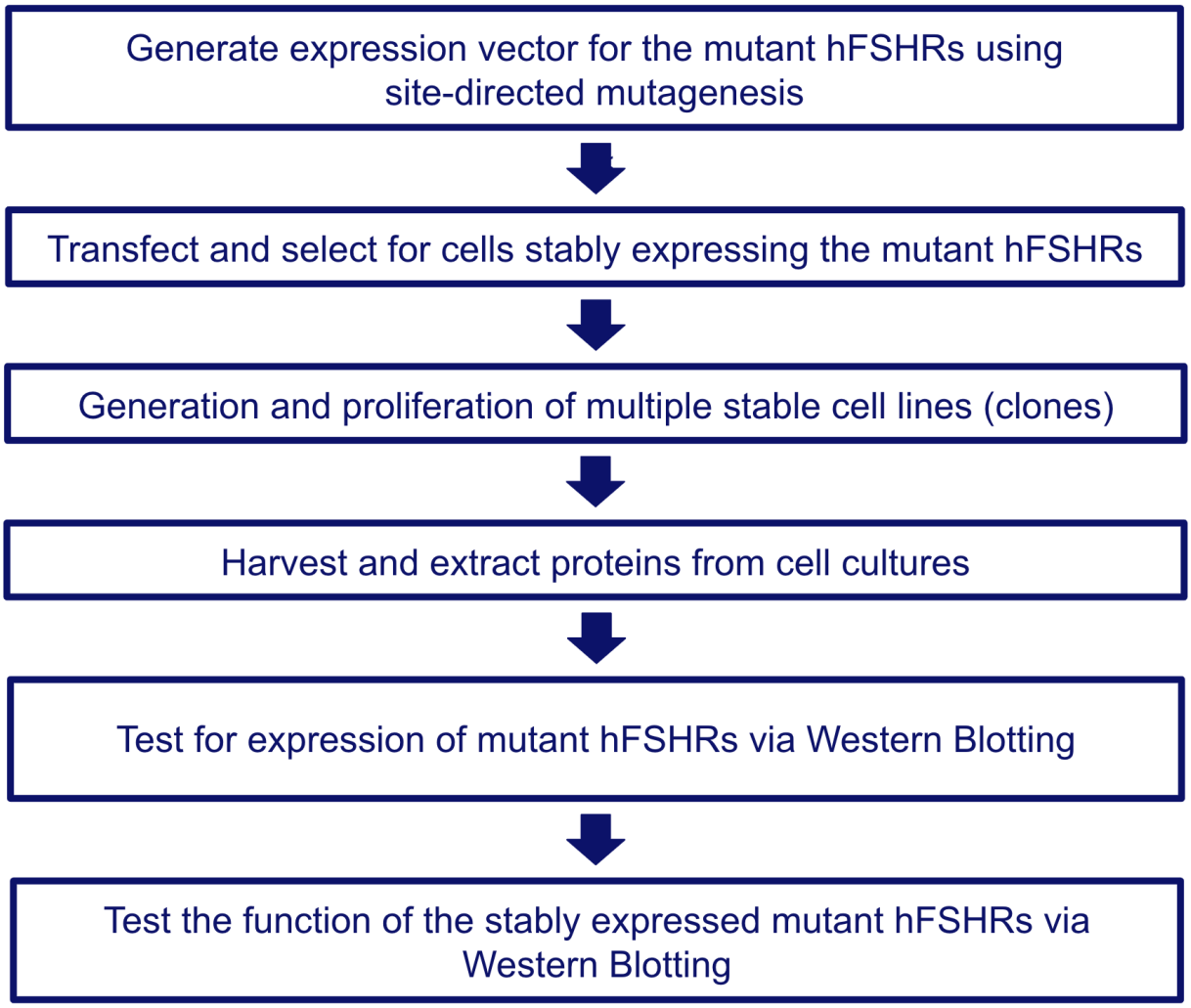


**Generation of Expression Vectors for Mutant hFSHRs:**

Mutations were induced in the FSHR CBM gene on the pIRESneo plasmid template using the Q5 site-directed mutagenesis kit protocol made by New England Biolabs (Figure 9).[15] The procedure utilizes a polymerase chain reaction with standard primers and Q5 DNA polymerase, followed by incubation with an enzyme mix of kinase, a ligase and DpnI. These enzymes allow for the PCR product to be quickly circularized and for the template DNA to be removed.[15] The standard primers, along with the low error rate of Q5 DNA polymerase, permits

the target sequence of DNA to be replicated with only the target mutations present. The plasmids formed from the PCR product were heat shocked for transformation and plate selection using the New England Biolabs 5-alpha Competent *E. coli* (High Efficiency) and chemically-competent cells, included with the kit.[15] By using this mutagenesis method, additional mutations were made on plasmid templates with pre-existing mutations. For example, the ABCD mutant was made by adding the 'D' mutation site onto the ABC mutant plasmid template.

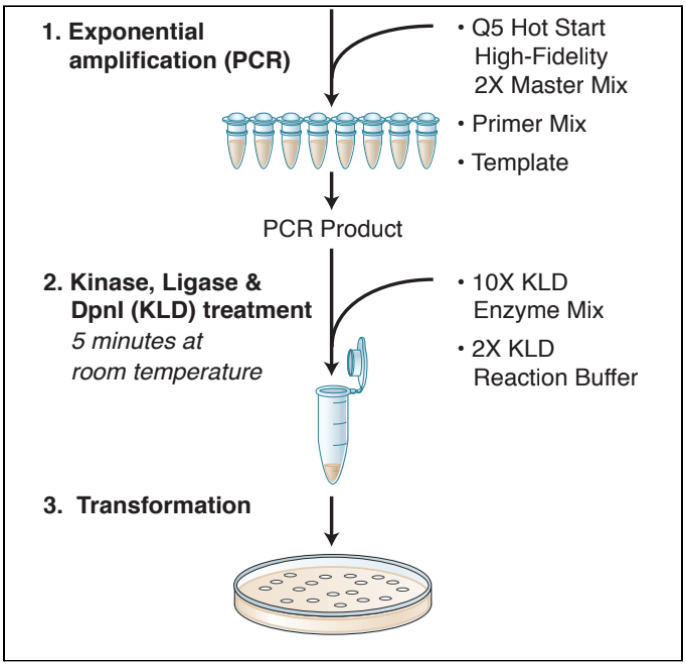


Figure 9. Schematic overview of the New England Biolabs Q5 site-directed mutagenesis procedure.[15]

**Confirmation of Mutant Identity via Restriction Digestion:**

In order to confirm the identity of the hFSHR mutants following the generation of the PCR product, a restriction digestion was used followed by visualization and analysis via agarose gel electrophoresis. When a mutation is made, an additional restriction site is included with the mutation. Thus, the presence of mutation sites can be confirmed when the plasmids are digested with the appropriate restriction enzymes since there will be an additional restriction site

associated with that added mutation site compared to the wild-type pIRESneo plasmid template. To detect the presence of the 'A' mutation site, there will be an additional BAMH1 site at 795 bp in the mutant plasmid compared to the wild-type. To detect the presence of the 'B' mutation site, there will be an additional NHE1 site at 7356 bp in the mutant plasmid compared to the wild-type, which does not have any NHE1 cut sites. To detect the presence of the 'C' mutation site, there will be an additional EAR1 site at 514 bp in the mutant plasmid compared to the wild-type. Additionally, there will be a shift in one of the EAR1 cut sites from 3081 bp in the wild-type to 2564 bp in the mutant. To detect the presence of the 'D' mutation site, there will be an additional AVRII site at 1104 bp in the mutant plasmid compared to the wild-type.

Following the New England Biolabs Restriction Digest protocol, the digestion reaction was set up, where the mutant plasmid DNA was mixed with 10X NEBuffer, DI water, and the appropriate restriction enzyme.[16] The reaction mixture was then incubated for one hour at 37℃ to allow for the digestion reaction to occur, followed by analysis via 2% agarose gel electrophoresis using the Team Cohen Master Lab Manual protocol.[17]

**Transfection and Selection of Stable Cell Lines:**

After the expression plasmids for the mutated FSHR isoforms were made, the mutants were stably transfected into human embryonic kidney 293 (HEK293) cells using the Mirus *Trans*IT®-293 Transfection Reagent protocol.[18] Following a 48-72 hour incubation period, the cells underwent a medium change to the G418 selection medium; the mutant plasmids contain a G418 selection marker so that cells that do not successfully take up and integrate the plasmid into the genome will die off. After 48-72 hours, colonies of cells that successfully took up the plasmid and thus survived selection by G418 were chosen for clonal expansion. The colonies

were picked up off of the plate using trypsinized disks and were moved to a 96-well plate, where each colony selected was placed in an individual well. Each colony, or clone, was expanded to larger well sizes as the cells grew, where stable expression of the hFSHR mutants was successfully achieved. Multiple clones or cell lines of each hFSHR mutant type were maintained in culture using T25 flasks. An overview for the transfection and generation of stably expressed mutant hFSHRs is represented in Figure 10.

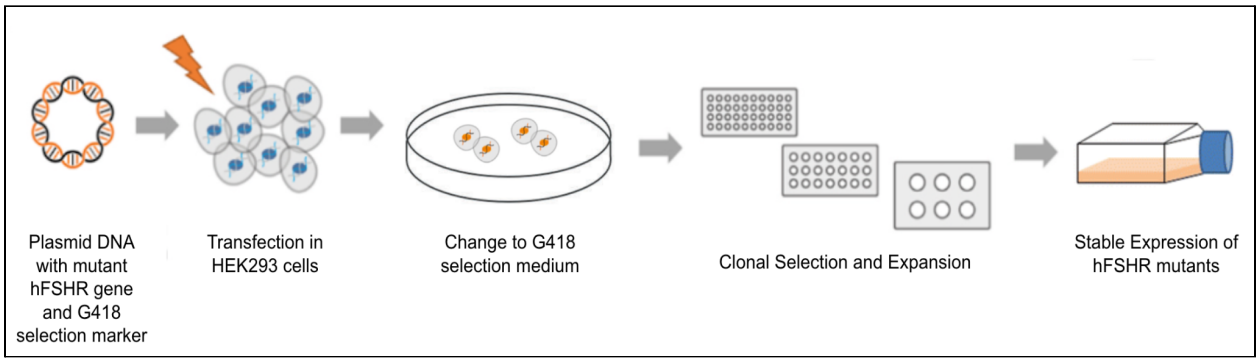


Figure 10. Schematic diagram for the transfection, selection, and expansion of stably expressed mutant hFSHRs. Multiple cell lines, or clones, were generated for each mutant type.[19]

**Extraction of Proteins from Cell Culture:**

To induce a starvation state and eliminate signaling activation prior to protein extraction, the cells were incubated at 37℃ for one hour in serum-free medium. The cells then underwent an FSH time course treatment, where FSH was added to each well at the following time points: 0, 5, 15, and 30 minutes. Following the FSH time course treatment, lysis buffer with a protease inhibitor and douncing were used to break apart the cell and release the proteins. Protein samples then underwent centrifugation at the 4ºC to separate and extract the protein from the cellular debris. The extracted protein fractions, containing hFSHR, were then tested for protein concentration using a bicinchoninic acid (BCA) assay.

**Quantification of Protein Concentration:**

In order to normalize the protein concentrations prior to western blotting, the protein concentrations were measured using the ThermoFisher Pierce™ BCA Protein Assay Kit.[20] The BCA assay standards were made following the kit protocol.[20] The protein fractions from each clone, measured in triplicates, were incubated in a 96-well plate with the BCA working reagent from the kit for 30 minutes at 37℃.[20] Following incubation, the protein concentrations were measured using a spectrophotometer at 562 nm. Protein concentrations were normalized to the protein sample with the lowest concentration, where the desired concentration was achieved for each sample by mixing calculated amounts of each protein fraction with 2x SDS sample buffer. The 2x SDS sample buffer was made following the Team Cohen Master Lab Manual.[17]

**Expression and Signaling Analysis via SDS-PAGE and Western Blotting:**

To separate the proteins present in each sample based on size, sodium dodecyl sulfate polyacrylamide gel electrophoresis (SDS-PAGE) was used following the procedure in the Team Cohen Master Lab Manual.[17] Following SDS-PAGE, the separated proteins were transferred to an Immobilon®-P PVDF transfer membrane using the BioRad semi-dry transfer method detailed in the Team Cohen Master Lab Manual (Figure 11).[17] The BioRad Trans-Blot SD Semi-Dry Transfer cell apparatus was used to perform the transfer.

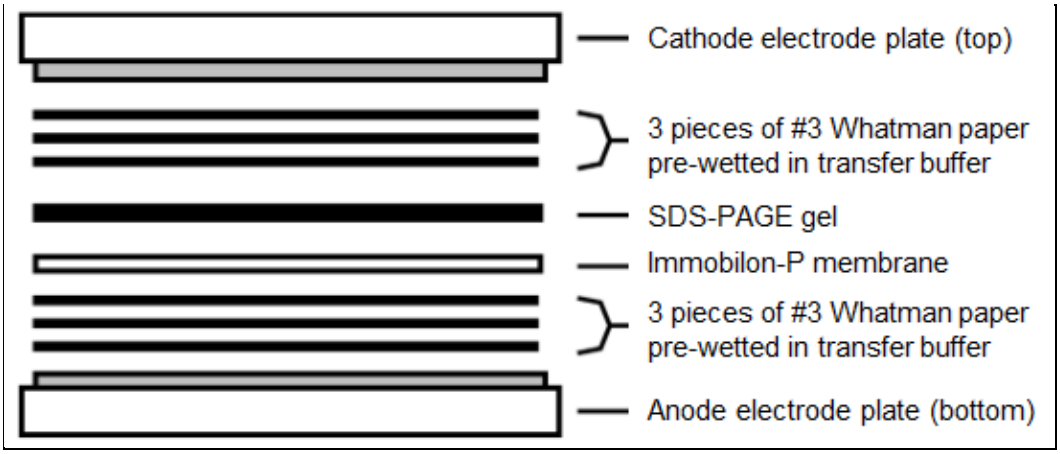


Figure 11. Schematic diagram for the set-up of the semi-dry transfer method using the BioRad Trans-Blot SD Semi-Dry Transfer cell.[17]

After the proteins were transferred to the Immobilon®-P PVDF transfer membrane, the membrane was blocked for one hour at room temperature on a rocker in a 5% BSA in 1x TBST solution indicated in the Team Cohen Master Lab Manual.[17] Following the 1-hour block, the membrane was incubated with the primary antibody overnight at 4°C. When testing for expression of hFSHR in the protein fraction, the primary antibody used was an anti-FSHR monoclonal antibody. When testing for signaling of hFSHR, the primary antibody used was a phospho-p44 antibody. After overnight incubation with the primary antibody, the membrane was washed with 1x TBST followed by a 1-hour incubation with the secondary antibody in a 5% milk in 1x TBST solution to probe for and bind to the primary antibody. When testing for expression of hFSHR in the protein fraction, the secondary antibody used was a goat anti-mouse IgG HRP antibody. When testing for signaling of hFSHR, the secondary antibody used was a goat anti-rabbit IgG HRP antibody. After the incubation with the secondary antibody, the membrane was washed with 1x TBST following a 5-minute incubation

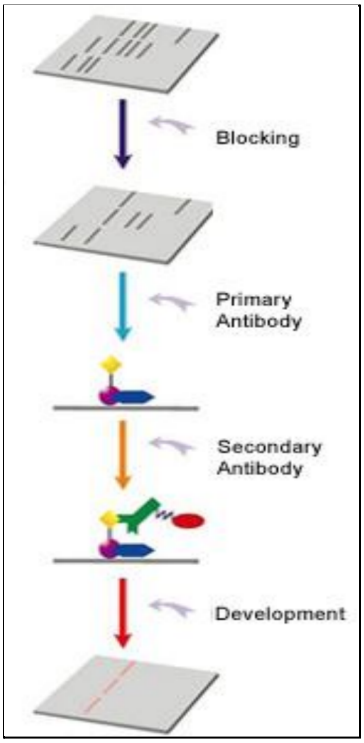


Figure 12. Overview of western blot detection procedure.[21]

with the ThermoFisher SuperSignal™ West Pico PLUS Chemiluminescent Substrate in order to detect bands using the BioRad ChemiDoc™ MP Imaging System. An overview of the western blotting detection procedure is shown in Figure 12.

## RESULTS

### Mutagenesis:

The mutants ABCD, ABC, and BCD were successfully made using site-directed mutagenesis. The ABCD mutant has the expected additional band at 795 bp when digested with BAMH1, thus confirming the presence of the 'A' mutation site (Figure 13, Table 1). The ABCD mutant has the expected band at 7356 bp when digested with NHE1, where the wild-type would not have any NHE1 cut sites at all, thus confirming the presence of of the 'B' mutation site in the ABCD mutant (Figure 13, Table 1). The ABCD mutant has the expected additional band at 514 bp as well as the shift from a band at 3081 bp in the wild-type to 2564 bp in the mutant when digested with EAR1, thus confirming the presence of of the 'C' mutation site (Figure 13, Table 1). Lastly, the ABCD mutant has the expected additional band at 1104 bp when digested with AVRII, thus confirming the presence of the 'D' mutation site (Figure 13, Table 1).

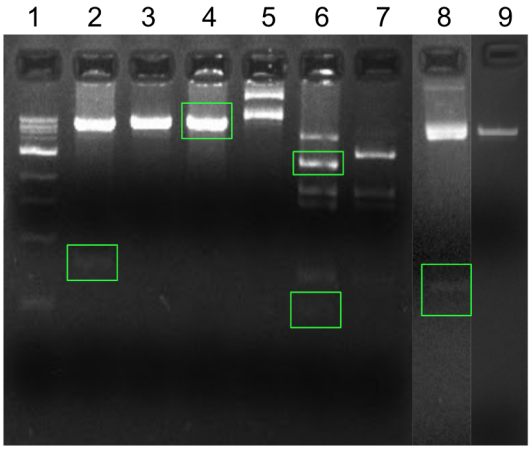


Figure 13. Agarose gel showing presence of mutation sites (A, B, C, and D) in the ABCD mutant. The corresponding restriction enzymes and samples shown for each lane can be found in Table 1.

Table 1. Presentation of mutations in ABCD mutants compared to WT. Samples, restriction enzymes, and expected bands (bp) for each lane shown in Figure 13.

| LANE | SAMPLE | MUTATION BEING CHECKED | ENZYME USED: | EXPECTED BANDS (bp) |
|---|---|---|---|---|
| 1 | MW | - | - | - |
| 2 | ABCD | A (F479L) | BAMH1 | 6561, 795 |
| 3 | WT | A (F479L) | BAMH1 | 7356 |
| 4 | ABCD | B (F481L) | NHE1 | 7356 |
| 5 | WT | B (F481L) | NHE1 | no cuts |
| 6 | ABCD | C (F486L) | EAR1 | **2564**, 1804, 1537, 724, **514**, 210 |
| 7 | WT | C (F486L)) | EAR1 | 3081, 1804, 1537, 724, 210 |
| 8 | ABCD | D (F489L) | AVRII | 6252, 1104 |
| 9 | WT | D (F489L) | AVRII | 7356 |

By the same reasoning for the ABCD mutant, the ABC mutant has the expected additional bands for the 'A,' 'B,' and 'C' mutation sites when digested with the respective restriction enzymes (Figure 14, Table 2). When digested with AVRII, the ABC mutant did not

have an additional band present at 1104 bp in the agarose gel, thereby presenting similar to the wild-type when digested with AVRII (Figure 14, Table 2). This result is expected, since the ABC mutant should not have a 'D' mutation site and should present like the wild-type when digested with AVRII. Thus, the ABC mutant was successfully created, as confirmed by the restriction digest results.

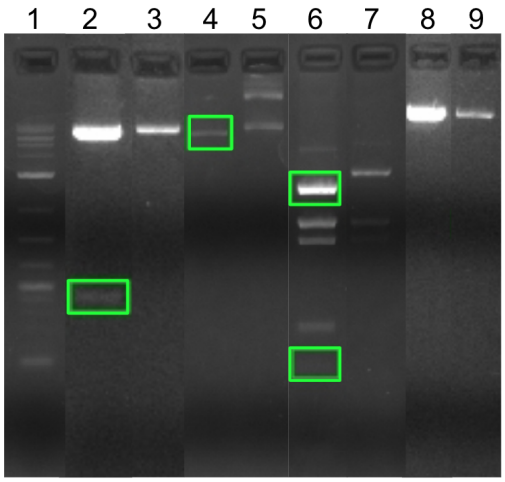


Figure 14. Agarose gel showing presence of mutation sites (A, B, and C) in the ABC mutant. The 'D' mutation site is absent in the ABC mutant. The corresponding restriction enzymes and samples shown for each lane can be found in Table 2.

Table 2. Presentation of mutations in ABC mutants compared to WT. Samples, restriction enzymes, and expected bands (bp) for each lane shown in Figure 14.

| LANE | SAMPLE | MUTATION BEING CHECKED | ENZYME USED | EXPECTED BANDS (bp) |
|---|---|---|---|---|
| 1 | MW | - | - | - |
| 2 | ABC | A (F479L) | BAMH1 | 6561, 795 |
| 3 | WT | A (F479L) | BAMH1 | 7356 |
| 4 | ABC | B (F481L) | NHE1 | 7356 |
| 5 | WT | B (F481L) | NHE1 | no cuts |
| 6 | ABC | C (F486L) | EAR1 | **2564**, 1804, 1537, 724, **514**, 210 |
| 7 | WT | C (F486L)) | EAR1 | 3081, 1804, 1537, 724, 210 |
| 8 | ABC | D (F489L) | AVRII | 7356 |
| 9 | WT | D (F489L) | AVRII | 7356 |

The BCD mutant has the expected additional bands for the 'B,' 'C,' and 'D' mutation sites when digested with the respective restriction enzymes (Figure 15, Table 3). When digested with BAMH1, the BCD mutant did not have an additional band present at 795 bp, thereby presenting similar to the wild-type when digested with BAMH1 (Figure 15, Table 3). This result is expected, since the BCD mutant should not have an 'A' mutation site and should present like the wild-type when digested with BAMH1.

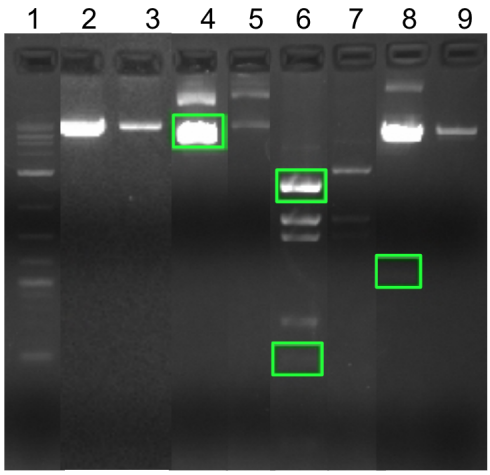


Figure 15. Agarose gel showing presence of mutation sites (B,C, and D) in the BCD mutant. The 'A' mutation site is absent in the BCD mutant. The corresponding restriction enzymes and samples shown for each lane can be found in Table 3.

Table 3. Presentation of mutations in BCD mutants compared to WT. Samples, restriction enzymes, and expected bands (bp) for each lane shown in Figure 15.

| LANE | SAMPLE | MUTATION BEING CHECKED | ENZYME USED: | EXPECTED BANDS (bp) |
|---|---|---|---|---|
| 1 | MW | - | - | - |
| 2 | BCD | A (F479L) | BAMH1 | 7356 |
| 3 | WT | A (F479L) | BAMH1 | 7356 |
| 4 | BCD | B (F481L) | NHE1 | 7356 |
| 5 | WT | B (F481L) | NHE1 | no cuts |
| 6 | BCD | C (F486L) | EAR1 | **2564**, 1804, 1537, 724, **514**, 210 |
| 7 | WT | C (F486L)) | EAR1 | 3081, 1804, 1537, 724, 210 |
| 8 | BCD | D (F489L) | AVRII | 6252, 1104 |
| 9 | WT | D (F489L) | AVRII | 7356 |

Double mutants (AB, BC, and CD) were also created in addition to the triple mutants (ABC, BCD) and the quadruple mutant (ABCD). The AB mutant has the expected additional bands for the 'A' (band at 795 bp) and 'B' (band at 7356 bp) mutation sites when digested with BAMH1 and NHE1, respectively (Figure 16, Table 4). When digested with EAR1 and AVRII, the AB mutant did not have additional bands present in the agarose gel, thereby presenting similar to the wild-type when digested with EAR1 and AVRII (Figure 16, Table 4). This result is expected, since the AB mutant should not have the 'C' and 'D' mutation sites and should present like the wild-type.

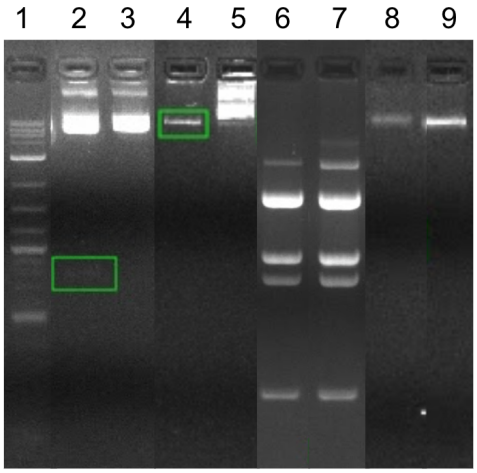


Figure 16. Agarose gel showing presence of mutation sites (A and B) in the AB mutant. The C and D mutation sites are absent in the AB mutant. The corresponding restriction enzymes and samples shown for each lane can be found in Table 4.

Table 4. Presentation of mutations in AB mutants compared to WT. Samples, restriction enzymes, and expected bands (bp) for each lane shown in Figure 16.

| LANE | SAMPLE | MUTATION BEING CHECKED | ENZYME USED: | EXPECTED BANDS (bp) |
|---|---|---|---|---|
| 1 | MW | - | - | - |
| 2 | AB | A (F479L) | BAMH1 | 6561, 795 |
| 3 | WT | A (F479L) | BAMH1 | 7356 |
| 4 | AB | B (F481L) | NHE1 | 7356 |
| 5 | WT | B (F481L) | NHE1 | no cuts |
| 6 | AB | C (F486L) | EAR1 | 3081, 1804, 1537, 724, 210 |
| 7 | WT | C (F486L)) | EAR1 | 3081, 1804, 1537, 724, 210 |
| 8 | AB | D (F489L) | AVRII | 7356 |
| 9 | WT | D (F489L) | AVRII | 7356 |

The BC mutant identity was confirmed as well, where the presence of the additional bands at 7356 bp when digested with NHE1 (‘B’ mutation site) and 2564 bp and 514 bp when digested with EAR1 (‘C’ mutation site) were shown in the agarose gel for the BC mutant (Figure 17, Table 5). When digested with BAMH1 (‘A’ mutation site) and AVRII (‘D’ mutation site), the BC mutant presented like wild-type (Figure 17, Table 5).

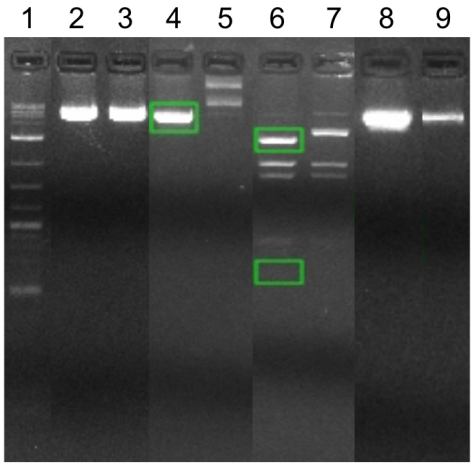


Figure 17. Agarose gel showing presence of mutation sites (B and C) in the BC mutant. The A and D mutation sites are absent in the BC mutant. The corresponding restriction enzymes and samples shown for each lane can be found in Table 5.

Table 5. Presentation of mutations in BC mutants compared to WT. Samples, restriction enzymes, and expected bands (bp) for each lane shown in Figure 17.

| LANE | SAMPLE | MUTATION BEING CHECKED | ENZYME USED: | EXPECTED BANDS (bp) |
|---|---|---|---|---|
| 1 | MW | - | - | - |
| 2 | BC | A (F479L) | BAMH1 | 7356 |
| 3 | WT | A (F479L) | BAMH1 | 7356 |
| 4 | BC | B (F481L) | NHE1 | 7356 |
| 5 | WT | B (F481L) | NHE1 | no cuts |
| 6 | BC | C (F486L) | EAR1 | **2564**, 1804, 1537, 724, **514**, 210 |
| 7 | WT | C (F486L)) | EAR1 | 3081, 1804, 1537, 724, 210 |
| 8 | BC | D (F489L) | AVRII | 7356 |
| 9 | WT | D (F489L) | AVRII | 7356 |

The expected additional bands for the ‘C’ and ‘D’ mutation sites were present when the CD mutant was digested with EAR1 and AVRII (Figure 18, Table 6). When digested with BAMH1 and NHE1, the CD mutant presented similar to wild-type in the agarose gel (Figure 18, Table 6).

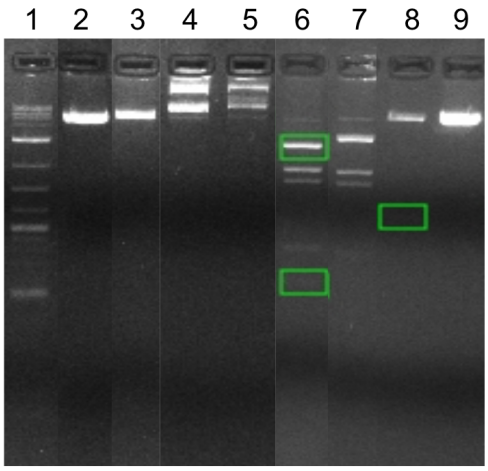


Figure 18. Agarose gel showing presence of mutation sites (C and D) in the CD mutant. The A and B mutation sites are absent in the CD mutant. The corresponding restriction enzymes and samples shown for each lane can be found in Table 6.

Table 6. Presentation of mutations in CD mutants compared to WT. Samples, restriction enzymes, and expected bands (bp) for each lane shown in Figure 18.

| LANE | SAMPLE | MUTATION BEING CHECKED | ENZYME USED: | EXPECTED BANDS (bp) |
|---|---|---|---|---|
| 1 | MW | - | - | - |
| 2 | CD | A (F479L) | BAMH1 | 7356 |
| 3 | WT | A (F479L) | BAMH1 | 7356 |
| 4 | CD | B (F481L) | NHE1 | no cuts |
| 5 | WT | B (F481L) | NHE1 | no cuts |
| 6 | CD | C (F486L) | EAR1 | **2564**, 1804, 1537, 724, **514**, 210 |
| 7 | WT | C (F486L)) | EAR1 | 3081, 1804, 1537, 724, 210 |
| 8 | CD | D (F489L) | AVRII | 6252, 1104 |
| 9 | WT | D (F489L) | AVRII | 7356 |

By the same reasoning for the quadruple, triple, and double mutants, the single mutants were created and their identity confirmed via agarose gel electrophoresis and restriction digestion. When digested with BAMH1, the A mutant had the additional band at 795 bp (Figure 19, Table 7). When digested with the other three enzymes, the A mutant presented similar to wild-type (Figure 19, Table 7). When digested with NHE1, the B mutant had the additional band at 7356 bp while the wild-type had no cuts (Figure 20, Table 8). When digested with the other three enzymes, the B mutant presented similar to wild-type (Figure 20, Table 8). When digested with EAR1, the C mutant had the additional band at 514 bp as well as the shift in band from 3081 bp to 2564 bp (Figure 21, Table 9). When digested with the other three enzymes, the C mutant presented similar to wild-type (Figure 21, Table 9). When digested with AVRII, the D

mutant has the additional band at 1104 bp in addition to presenting similar to wild-type when digested with the other three enzymes (Figure 22, Table 10).

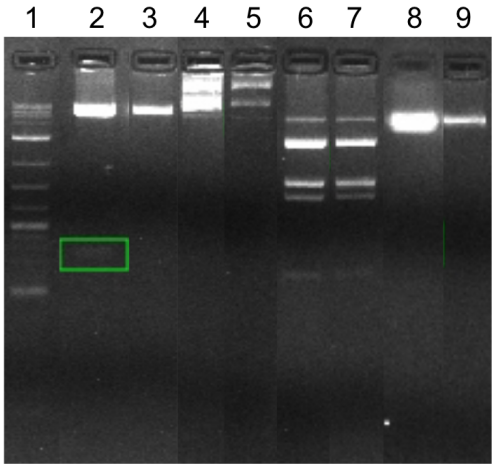


Figure 19. Agarose gel showing presence of mutation site (A) in the A mutant. The B, C, and D mutation sites are absent in the A mutant. The corresponding restriction enzymes and samples shown for each lane can be found in Table 7.

Table 7. Presentation of mutations in A mutants compared to WT. Samples, restriction enzymes, and expected bands (bp) for each lane shown in Figure 19.

| LANE | SAMPLE | MUTATION BEING CHECKED | ENZYME USED: | EXPECTED BANDS (bp) |
|---|---|---|---|---|
| 1 | MW | - | - | - |
| 2 | A | A (F479L) | BAMH1 | 6561, 795 |
| 3 | WT | A (F479L) | BAMH1 | 7356 |
| 4 | A | B (F481L) | NHE1 | no cuts |
| 5 | WT | B (F481L) | NHE1 | no cuts |
| 6 | A | C (F486L) | EAR1 | 3081, 1804, 1537, 724, 210 |
| 7 | WT | C (F486L)) | EAR1 | 3081, 1804, 1537, 724, 210 |
| 8 | A | D (F489L) | AVRII | 7356 |
| 9 | WT | D (F489L) | AVRII | 7356 |

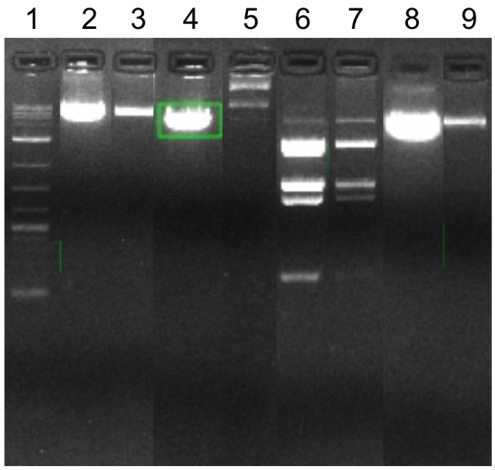


Figure 20. Agarose gel showing presence of mutation site (B) in the B mutant. The A, C, and D mutation sites are absent in the B mutant. The corresponding restriction enzymes and samples shown for each lane can be found in Table 8.

Table 8. Presentation of mutations in B mutants compared to WT. Samples, restriction enzymes, and expected bands (bp) for each lane shown in Figure 20.

| LANE | SAMPLE | MUTATION BEING CHECKED | ENZYME USED: | EXPECTED BANDS (bp) |
|---|---|---|---|---|
| 1 | MW | - | - | - |
| 2 | B | A (F479L) | BAMH1 | 7356 |
| 3 | WT | A (F479L) | BAMH1 | 7356 |
| 4 | B | B (F481L) | NHE1 | 7356 |
| 5 | WT | B (F481L) | NHE1 | no cuts |
| 6 | B | C (F486L) | EAR1 | 3081, 1804, 1537, 724, 210 |
| 7 | WT | C (F486L)) | EAR1 | 3081, 1804, 1537, 724, 210 |
| 8 | B | D (F489L) | AVRII | 7356 |
| 9 | WT | D (F489L) | AVRII | 7356 |

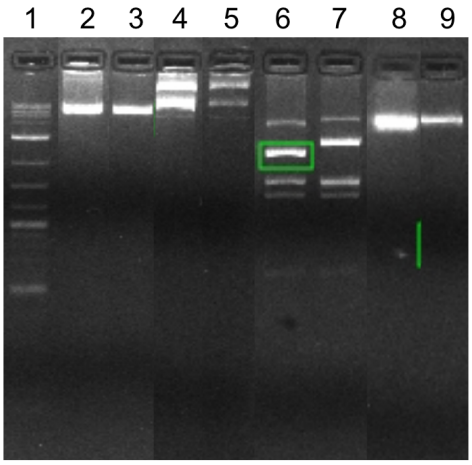


Figure 21. Agarose gel showing presence of mutation site (C) in the C mutant. The A, B, and D mutation sites are absent in the C mutant. The corresponding restriction enzymes and samples shown for each lane can be found in Table 9.

Table 9. Presentation of mutations in C mutants compared to WT. Samples, restriction enzymes, and expected bands (bp) for each lane shown in Figure 21.

| LANE | SAMPLE | MUTATION BEING CHECKED | ENZYME USED: | EXPECTED BANDS (bp) |
|---|---|---|---|---|
| 1 | MW | - | - | - |
| 2 | C | A (F479L) | BAMH1 | 7356 |
| 3 | WT | A (F479L) | BAMH1 | 7356 |
| 4 | C | B (F481L) | NHE1 | no cuts |
| 5 | WT | B (F481L) | NHE1 | no cuts |
| 6 | C | C (F486L) | EAR1 | **2564**, 1804, 1537, 724, **514**, 210 |
| 7 | WT | C (F486L)) | EAR1 | 3081, 1804, 1537, 724, 210 |
| 8 | C | D (F489L) | AVRII | 7356 |
| 9 | WT | D (F489L) | AVRII | 7356 |

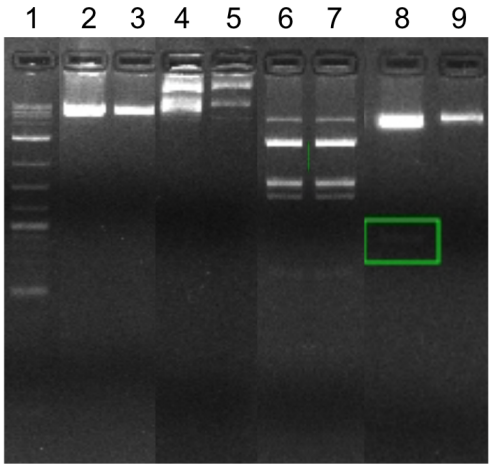


Figure 22. Agarose gel showing presence of mutation site (D) in the D mutant. The A, B, and C mutation sites are absent in the D mutant. The corresponding restriction enzymes and samples shown for each lane can be found in Table 10.

Table 10. Presentation of mutations in D mutants compared to WT. Samples, restriction enzymes, and expected bands (bp) for each lane shown in Figure 22.

| LANE | SAMPLE | MUTATION BEING CHECKED | ENZYME USED: | EXPECTED BANDS (bp) |
|---|---|---|---|---|
| 1 | MW | - | - | - |
| 2 | D | A (F479L) | BAMH1 | 7356 |
| 3 | WT | A (F479L) | BAMH1 | 7356 |
| 4 | D | B (F481L) | NHE1 | no cuts |
| 5 | WT | B (F481L) | NHE1 | no cuts |
| 6 | D | C (F486L) | EAR1 | 3081, 1804, 1537, 724, 210 |
| 7 | WT | C (F486L)) | EAR1 | 3081, 1804, 1537, 724, 210 |
| 8 | D | D (F489L) | AVRII | 6252, 1104 |
| 9 | WT | D (F489L) | AVRII | 7356 |

## Expression of Mutant hFSHR in the Transfected Cell:

Following extraction of proteins from cell culture and protein concentration quantification, hFSHR expression in the ABCD, ABC, and BCD was determined via SDS-PAGE and western blotting in order to determine the success of the stable transfections (Figure 23). Two clones of each mutant were tested for expression in order to further confirm the success and

repeatability of the stable transfections. By probing with an anti-FSHR monoclonal antibody, expression of the hFSHR protein in the ABCD, ABC, and BCD mutants were shown by the presence of a doublet band around 76 kDa, which is the molecular weight of hFSHR (Figure 23).

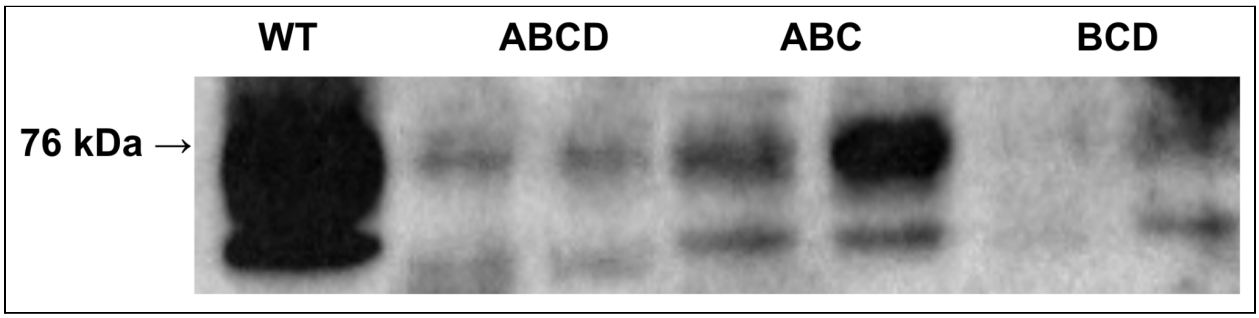


Figure 23. Western blot showing expression of wild type (WT) FSHR and the stably expressed FSHR mutants. Expression was detected using anti-FSHR monoclonal antibody.

**Signaling of Mutant hFSHRs:**

Signaling of the mutant hFSHRs was tested via SDS-PAGE and western blotting following a time course of FSH treatment. The western blots were probed with an anti-phospho-p44 antibody in order to measure changes in signaling in the ERK 1/2 pathway, also known as the p44/42 MAPK pathway. Band darkness when probed with phospho-p44 is indicative of the level of signaling. In the wild-type hFSHR, signaling increases at 5 minutes and decreases at the 15 and 30 minute FSH treatment time points (Figure 24). In the ABCD, ABC, and BCD mutant hFSHRs, signaling at the 0 minute FSH treatment time point is greater than that of wild-type (Figure 24). Signaling at 5 minutes in all three mutant hFSHRs is also greater than the wild-type at 5 minutes, where the level of signaling remains high at the 15 and 30 minute time points while signaling decreases in the wild-type (Figure 24). APPL1 was used as a loading control to ensure that the differences in band darkness in the blots are due to differences in signaling and not due to unequal loading. The band darkness was found to be equal across all lanes in the loading control (Figure 24).

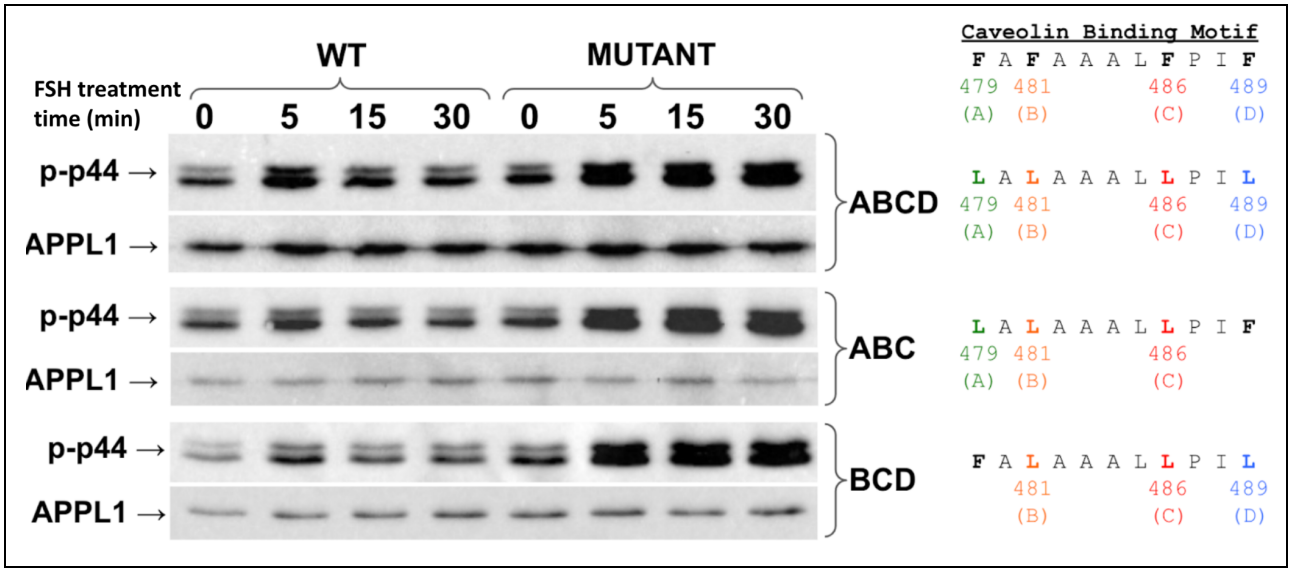


Figure 24. Western blots showing signaling time course treatment of WT FSHR and the mutant FSHRs (ABCD, ABC, BCD), probed with anti-phospho-p44 antibody. The time (0, 5, 15, 30 minutes) that FSHR is exposed to FSH ligand is indicated for each sample. Loading control (APPL1) for each mutant is shown. The corresponding mutations in the CBM for each mutant are shown to the right of the blots.

## DISCUSSION

The mutagenesis for the quadruple (ABCD), triple (ABC, BCD), double (AB, BC, CD), and single (A, B, C, D) mutants was successful, where the identity of all mutants were confirmed via restriction digestion and agarose gel electrophoresis (Figures 13-22). Stable transfections of the quadruple, triple, and double mutants were attained with multiple clones of each mutant as well, where the ABCD, ABC, and BCD mutants were chosen to continue with further testing. The ABCD, ABC, and BCD mutants were found to successfully express the mutant hFSHR via western blotting (Figure 23). Two clones of each mutant were confirmed to express the mutant hFSHR.

In terms of signaling, the quadruple and triple mutant hFSHRs were found to have significant differences in signaling compared to the wild-type. The ABCD, ABC, and BCD mutants presented similarly in their signaling. Basal activation was increased in the mutant hFSHRs, as indicated by the darker band at the 0 minute time point (Figure 24). Signaling was also found to be increased at the 5, 15, and 30 minute time points, thus indicating that the mutant hFSHRs have increased signaling of the ERK 1/2 pathway as well as persistent signaling following the peak of signaling at the 5 minute time point seen in the wild-type hFSHR (Figure 24). Thus, the hypothesis that mutating the caveolin binding motif will affect hFSHR signaling is supported by the signaling data.

Because the signaling of these three mutants (ABCD, ABC, BCD) were similar, it was concluded that the mutation sites B (F481L) and C (F486L) in the CBM affect binding to caveolin, since the B and C sites were the only two mutations conserved across ABCD, ABC, and BCD. It is also important to note that the B mutation site is located on the opposite side of the helical wheel compared to the A (F479L), C (F486L), and D (F489L) mutation sites,

providing insight as to the side of the alpha helix or location in the CBM where caveolin directly interacts with hFSHR (Figure 6).

Based on the increased signaling of the mutant hFSHRs, it is predicted that hFSHR interaction with caveolin in lipid rafts via the CBM is responsible for regulating signaling, where disrupting the CBM may prevent hFSHR recruitment to the lipid raft. Wild-type hFSHR resides in lipid rafts and leaves the raft to signal after binding to hFSH. Based on these findings, we now predict that hFSHR is targeted to the lipid rafts by caveolin through the CBM of the hFSHR. Lipid rafts act in an inhibitory manner to regulate hFSHR signaling when hFSHR is targeted to the lipid rafts.. Without the ability to bind to caveolin, mutant hFSHRs cannot be targeted to lipid rafts for regulation and instead remain outside of the raft, where arrestin-dependent signaling can occur (Figure 25). If the mutant hFSHRs remain outside of the lipid raft, they are more accessible by arrestin and are thus internalized at a faster rate, thereby explaining the increase in signaling compared to the wild-type hFSHRs seen in the western blot analysis (Figure 24).

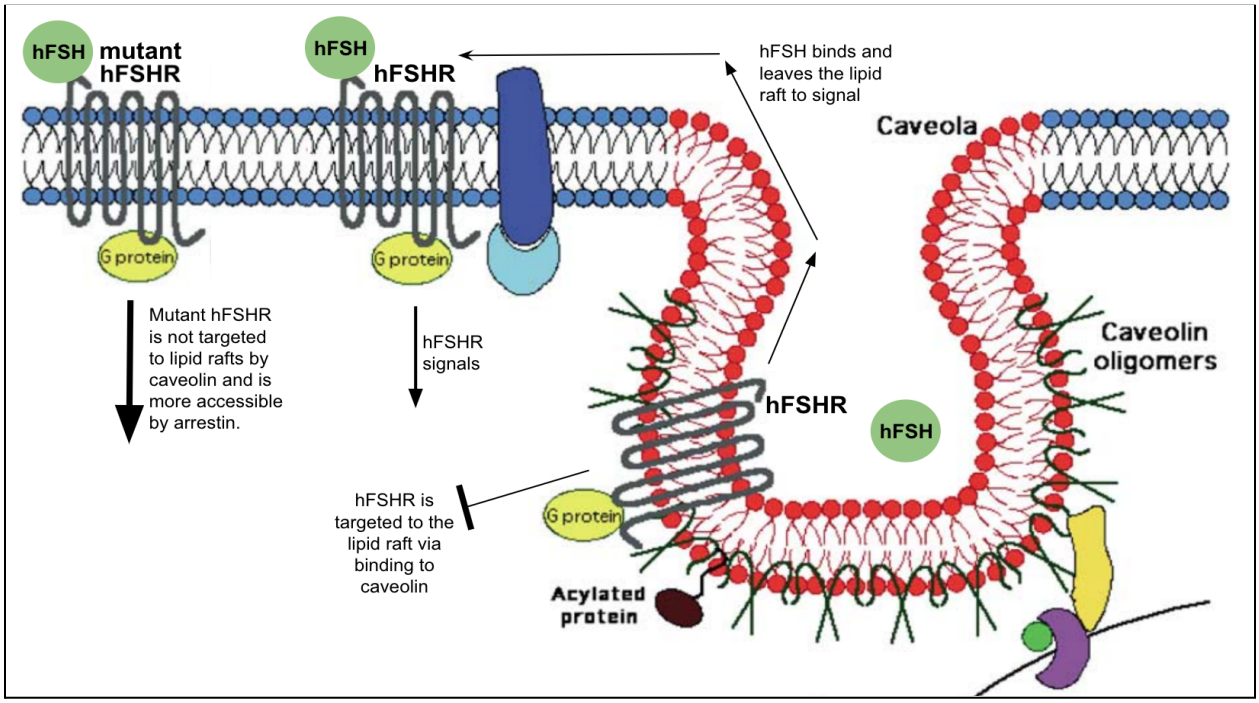


Figure 25. After hFSH binds, hFSHR leaves the lipid raft. Caveolin targets hFSHR to lipid rafts, where signaling is regulated.[22]

## FUTURE DIRECTIONS

Future research includes determining the importance of the 'B' (F481) and 'C' (F486) mutation sites of the CBM in affecting hFSHR signaling, since the conserved mutation sites in the ABCD, ABC, and BCD mutants were the 'B' and 'C' mutation sites. By testing and comparing the signaling of the double mutants (AB, BC, and CD) and the single mutants (A, B, C, and D), a greater understanding of which mutations in the CBM are important for proper hFSHR function can be attained. Additional experiments involving co-immunoprecipitation may also be beneficial in determining if the the mutations in the CBM alter hFSHR interaction with caveolin, rather than just altering signaling as shown in the presented data. Future experiments such as a sucrose gradient are proposed as well in order to reveal if there is a difference in hFSHR raft residency due to the mutations in the CBM.

## CONCLUSIONS

Not only were the quadruple, triple, and double mutants successfully created and stably transfected into HEK293 cells, but the increased signaling of the quadruple and triple mutants revealed the importance of the CBM in hFSHR and its interaction with caveolin in regulating signaling via targeting to lipid rafts. Future experiments are needed in order to further elucidate the specifics as to what parts of the CBM inform proper hFSHR function as well as potential differences in hFSHR interaction with caveolin and the lipid raft due to mutations in the CBM. A greater understanding of the interaction between FSHR and caveolin is beneficial in learning about how defects in FSHR function can cause infertility. By mutating the CBM of FSHR, the knowledge gained from the specifics of these mutations can be used to potentially develop pharmaceuticals that target the CBM in order to promote increased signaling, thus allowing for

the development of better assisted reproductive technologies or more accessible infertility treatments.

## ACKNOWLEDGEMENTS

I would like to thank Professor Brian Cohen for believing in me as I pursued this research, where his guidance and mentorship throughout my time at Union has allowed me to successfully complete this project. I would also like to thank the members of Team Cohen for their collaboration and support on my thesis and in life. I would like to thank the Union College Biochemistry program, Biology Department, Davenport Summer Research Fellowship, Faculty Research Grant, and Student Research Grant for the necessary funding for this project. Lastly, I would like to thank my family and friends for the countless hours of support and encouragement that they provided me during my time performing research at Union.

## REFERENCES


1. Dias, J. A., Cohen, B. D., Lindau-Shepard, B., Nechamen, C. A., Peterson, A. J., & Schmidt, A. (2002). Molecular, structural, and cellular biology of follitropin and follitropin receptor. *Vitamins and hormones*, 64, 249–322. https://doi.org/10.1016/s0083-6729(02)64008-7
2. Tran, S., Zhou, X., Lafleur, C., Calderon, M. J., Ellsworth, B. S., Kimmins, S., Boehm, U., Treier, M., Boerboom, D., & Bernard, D. J. (2013). Impaired fertility and FSH synthesis in gonadotrope-specific Foxl2 knockout mice. *Molecular endocrinology (Baltimore, Md.)*, 27(3), 407–421. https://doi.org/10.1210/me.2012-1286
3. Matzuk, M. M., & Lamb, D. J. (2008). The biology of infertility: research advances and clinical challenges. *Nature medicine*, 14(11), 1197–1213. https://doi.org/10.1038/nm.f.1895
4. "Infertility." Newsroom Fact Sheets, World Health Organization. 2020. Retrieved from www.who.int/news-room/fact-sheets/detail/infertility
5. "Infertility FAQs." Division of Reproductive Health, National Center for Chronic Disease Prevention and Health Promotion. 2019.
6. Ulloa-Aguirre, A., Reiter, E., & Crépieux, P. (2018). FSH Receptor Signaling: Complexity of Interactions and Signal Diversity. *Endocrinology*, 159(8), 3020–3035. https://doi.org/10.1210/en.2018-00452
7. Casarini, L., & Crépieux, P. (2019). Molecular Mechanisms of Action of FSH. *Frontiers in endocrinology*, 10, 305. https://doi.org/10.3389/fendo.2019.00305
8. García Cordero, J., León Juárez, M., González-Y-Merchand, J. A., Cedillo Barrón, L., & Gutiérrez Castañeda, B. (2014). Caveolin-1 in lipid rafts interacts with dengue virus NS3

during polyprotein processing and replication in HMEC-1 cells. *PloS one*, 9(3), e90704. https://doi.org/10.1371/journal.pone.0090704

9. Hernaiz-Llorens, M., Martínez-Mármol, R., Roselló-Busquets, C., & Soriano, E. (2021). One Raft to Guide Them All, and in Axon Regeneration Inhibit Them. *International journal of molecular sciences*, 22(9), 5009. https://doi.org/10.3390/ijms22095009
10. Ishikawa, Y., Cho, G., Yuan, Z., Inoue, N., & Nakae, Y. (2006). Aquaporin-5 water channel in lipid rafts of rat parotid glands. *Biochimica et biophysica acta*, 1758(8), 1053–1060. https://doi.org/10.1016/j.bbamem.2006.03.026
11. Martinez-Outschoorn, U. E., Sotgia, F., & Lisanti, M. P. (2015). Caveolae and signalling in cancer. *Nature reviews. Cancer,* 15(4), 225–237. https://doi.org/10.1038/nrc3915
12. Insel, P. A., Head, B. P., Patel, H. H., Roth, D. M., Bundey, R. A., & Swaney, J. S. (2005). Compartmentation of G-protein-coupled receptors and their signalling components in lipid rafts and caveolae. *Biochemical Society transactions*, 33(Pt 5), 1131–1134. https://doi.org/10.1042/BST20051131
13. Pérez-Verdaguer, M., Capera, J., Martínez-Mármol, R., Camps, M., Comes, N., Tamkun, M. M., & Felipe, A. (2016). Caveolin interaction governs Kv1.3 lipid raft targeting. *Scientific reports*, 6, 22453. https://doi.org/10.1038/srep22453
14. Dart C. (2010). Lipid microdomains and the regulation of ion channel function. The *Journal of physiology,* 588(Pt 17), 3169–3178. https://doi.org/10.1113/jphysiol.2010.191585
15. "Q5 Site-Directed Mutagenesis Kit Instruction Manual." New England Biolabs. 2022.
16. "Restriction Digest Protocol." New England Biolabs. 2022.
17. "Team Cohen Master Lab Manual." Team Cohen. 2022.

18. “TransIT®-293 Transfection Reagent Protocol.” Mirus. 2022.
19. Luthra, A., Spanjaard, R. A., Cheema, S., Veith, N., Kober, L., Wang, Y., Jing, T., Zhao, Y., Hoeksema, F., Yallop, C., Havenga, M., & Bakker, W. (2021). STEP® vectors for rapid generation of stable transfected CHO cell pools and clones with high expression levels and product quality homogeneity of difficult-to-express proteins. *Protein expression and purification*, 186, 105920. https://doi.org/10.1016/j.pep.2021.105920
20. “Pierce™ BCA Protein Assay Kit User Guide (Microplate Procedure).” ThermoFisher. 2022.
21. “One-Step Western™ Blot Manual.” GenScript. 2022.
22. Ostrom, R. S., & Insel, P. A. (2004). The evolving role of lipid rafts and caveolae in G protein-coupled receptor signaling: implications for molecular pharmacology. *British journal of pharmacology*, 143(2), 235–245. https://doi.org/10.1038/sj.bjp.0705930